Locating the Wood Defects with Typical Features and SVM

Zhao Zhang, Ning Ye, Dongyang Wu, Qiaolin Ye
School of Information Technology, NanJing Forestry University
NanJing, 210037, China
E-mail: zhangzhao_618@163.com

Abstract

Local Binary Pattern (LBP) can provide us with the spatial structure of images and describe the original features better, such as curly edges, etc. And it has better luminance adaptability. Dual-Tree Complex Wavelet Transform (DTCWT) can maintain better time-frequency localized characteristics and extract the energy based statistical features, maintaining the limited data redundancy and effectual computation efficiency.

Furthermore, the values of a board have a direct relationship with the grading determined by the defects on wood surfaces and determine the potential uses and the values for the Sawmills. In this paper, we effectively integrated the features by LBP and DTCWT to get the typical features for recognition. We proposed a wood defects recognition algorithm, which can effectively decrease the experimental errors and have better robust to the interferences. The method has been tested with color wood images. Based on visual valuation, the errors are relatively lower. After many comparative experiments, the results show the system is effectual and practical with better research values and potential applications.

Key Words: SVM; Dual-Tree Complex Wavelet Transform; Local Binary Pattern; Wood Defect Recognition; Texture Analysis

1 Introduction

Feature extraction plays an important role in pattern analysis. Many object surfaces show some texture characteristics, such as coarse, confusion, etc. At the time, the classification bases will be based on it rather than the uniformity of intensity, just like wood defects, the types and distribution of which vary. In the researches, it's impossible to extract all the texture characteristics of defects and the system suffers from the variations in the materials, causing selecting typical features for classification is difficult.

However, woods are the indispensable important resources and much in demand. However, the coverage of forests reduces substantially. In view of it, the rational uses of woods are the first measures be taken. Currently, how to improve the utilization rate of woods effectively is on a hot. In the production, the defects need to be removed. However, in most countries, this work is mainly finished by workers, costing many resources. Provided we can achieve accurate positioning and handling to the defects by the machines, we can improve the utilization rate of boards and avoid the wastes.

At present, some researchers have begun to study the solution measures. Finn Matti Niskanen [1] and their group adopt SOM to study color and texture based wood defect detection problems. The recognition mainly depends on color and texture characteristics. However, the system is vulnerable to thick dots on wood surfaces and the errors are relatively higher. In addition, German P. Meinlschmidt [2] and their group adopt infrared thermal imaging technology to study wood materials based defect detection problems. In their experiments, the materials under inspection are heated with radiators and the bases are the temperature above defects decreases slower than other regions. They complete defect detection online, however, the system costs more runtime and can only for special purposes, the practical value of which is relatively lower.

In fact, many researches indicate no one feature extraction technology is absolutely better than another, appropriate combination of them can obtain better recognition results. This paper adopts DTCWT and LBP to extract the features named the united statistical features by LBP and DTCWT (USF-LDT). Finally, we received a better identification effect and the system had better robust, raising the accuracy effectively.

And the diagram of SVM based classifier is presented in Figure 1-1.

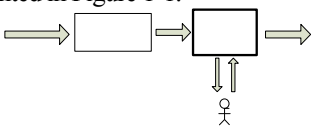

Figure 1-1. The block diagram of SVM based detection classifier.

2 Wood representation by USF-LDT

Kingsbury [5, 7, 8] proposed the DTCWT, which is composed by two biorthogonal filters and has better direction selective. The features based on en energy by DTCWT can be used to capture the wood texture characteristics, making it can effectively portray the global features, but the structure of it could not be described well.

However, LBP [3, 9] provides the spatial structure of the current image and LBP code was invariant to monotonous gray and was a texture descriptor which codified local primitives of the wood texture, such as curved edges, spots, etc. into LBP feature histograms [4]. Next, we will illuminate the different roles of LBP local and DTCWT global features.

2.1 Description of LBP texture features

LBP is put forward by Ojala [4] et al and LBP code determined by n sample points is used. For the fixed pixel centre coordinates (x_d, y_d), LBP is defined as a binary contrast between center pixel and the n surrounding pixels. Texture W is defined as the united distribution of the gray levels of n pixels: $W=w(i_c,i_1,...,i_n)$, where, i_c corresponds the gray value of the center pixel. i_n （n=1, 2,…,P）corresponds the gray value of the n equally spaced pixels on a circle of radius R (R>0) that forms a circularly symmetric set.

The coordinates of the n neighbors of the center pixel in the edge of the circle R can be calculated as following:

$$(x_n, y_n) = \left[x_d + R\cos(\frac{2\pi n}{P}), y_d + R\sin(\frac{2\pi n}{P}) \right] \quad (2.1)$$

To achieve invariant with respect to any monotonic transformation, only the signs of the differences were considered:

$$W \approx w(scale(i_1 - i_c),...,scale(i_n - i_c)) \quad , \quad \text{where,}$$

$$scale(a) = \begin{cases} 0, a < 0 \\ 1, a \geq 0 \end{cases} \quad (2.2)$$

A binomial weight 2^n will be assigned to each sign $scale(i_n - i_c)$ and transform the differences into a unique LBP code:

$$LBP_{P,R}(x_d, y_d) = \sum_{n=1}^{n} scale(i_n - i_c)2^n \quad (2.3)$$

Here, we adopt uniform $LBP_{P,R}^{u2}$ of values (*P*, *R*) equal to (8, 1), i.e. around a circle of radius R were eight adjacent pixels and the mapping type was uniform. In the experiments, the feature set selection is very important. After many cross experiments, we select all the feature sets with pixels 30*30.

In the feature extraction, we divide the wood images into three layers of R,G,B and divide each layer into many small blocks. Next, we extract the 59 dimension features denoted by LBP histograms from each block, marked by LBR, LBG and LBB separately.

Finally, the dimensions of the features are reduced to 1*177, represented by LBF. The LBP texture feature extraction process is shown in Figure3-1.

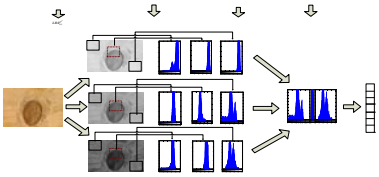

Figure2-1.LBP feature extraction process.

2.2 Description of DTCWT features

Kingsbury [5, 6] proposed the DTCWT [7, 8] and it can maintain limited data redundancy.

Provided the low-pass filters and high-pass filters of wavelet decomposition are respectively defined as $H_0(z)$, $H_1(z)$, while the reconstruction filters can be defined as $H_0(z^{-1})$ and $H_1(z^{-1})$.

For input signal $X(z)$, the low-pass and high-pass coefficients can be represented as following:

$$C^j(z^{2^j}) = \frac{1}{2^j}\sum_{k=0}^{2^j-1} X(w_{2^j}^k z) A(w_{2^j}^k z) \quad (2.4)$$

$$D^j(z^{2^j}) = \frac{1}{2^j}\sum_{k=0}^{2^j-1} X(w_{2^j}^k z)B(w_{2^j}^k z) \quad (2.5)$$
$$= \frac{1}{2^j}\sum_{k=-2^{j-1}}^{2^{j-1}-1} X(w_{2^j}^k z)B(w_{2^j}^k z), j = 1,2,...,J$$

Hence, the signal $X(z)$ can be decom -posed into:

$$X(z) = X_l^J + \sum_{j=0}^{J} X_h^h(z) \quad (2.6)$$
$$= C^j(z^{2^j})A^j(z^{-1}) + \sum_{j=1}^{J} D^j(z^{2^j})B^j(z^{-1})$$
$$= X_l^J + \sum_{j=1}^{J}\frac{1}{2^j}\sum_{k=-2^{j-1}}^{2^{j-1}-1} X(w_{2^j}^k z)B(w_{2^j}^k z)B(z^{-1})$$

Here, three-level wavelet transform is adopted. In DTCWT feature selection [10, 11,12] process, the feature set is defined as $\theta=\{S_i^j, P_i^j, \mu_i, \delta_i\}$, where, i=1,2, …,6, representing six complex wavelet sub-bands, where l = 1,2,…, L and μ, σ are the mean and standard deviation. Finally,19*2 dimensional feature vectors are regarded as the result represented by DTW_F expressed as the following:

$$\sum_{i_1=1}^{6}(FV\_e(i_1), FV\_std(i_1)) + \sum_{i_2=1}^{6}(FV\_e(i_2), FV\_std(i_2))$$
$$+\sum_{i_3=1}^{6}(FV\_e(i_3), FV\_std(i_3)) + \sum_{i=1}(FV\_e(i), FV\_std(i))$$

Where, FV_e is the mean, FV_std stands for standard deviation and i_1 , i_2 , i_3 are the number of high-frequent sub-bands and i represents low-frequent sub-bands. The extraction process is illustrated in Figure 2-2.

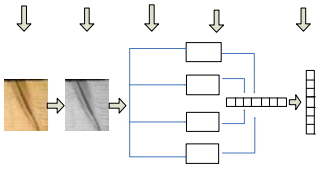

Figure2-2.DTCWT feature extraction process.

2.3 Description of the typical features

Finally, we aggregately obtain 215 dimension eigenvectors. As above explanation, the two sets contain different features for recognition.

Considering the typical features based classifier is generally superior to single and has enough error diversity, we combine LBF with DTW_F to improve the system performance. Hence, the SVM model trained has large diversity in error when facing the diversified interferential information.

Figure 2-3 illustrates the typical features combination process.

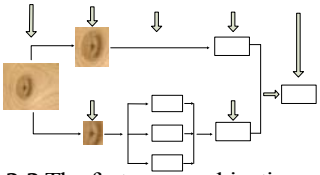

Figure 2-3. The features combination process.

As above-mentioned, DTW_F described the global features, thus better for coarse representation, while LBF captured the details in local areas, thus better for finer representation.

3 Performance Standards

For the tests, the number of detection produced in the system is defined as N_sum. The number of incision on the real defects is defined as N_labeled. The number of incision to the detected and labeled defects in the identification is defined as N_dlabeled and the number of misjudging defects as normal and misjudging sound woods as defects is defined as DN_sum and SD_sum respectively.

The *Missed rates*（*M1*）indicate the proportion of the missed defects to real labeled defects and can be determined by:

$$M1 = \frac{N\_labeled - N\_dlabeled}{N\_labeled} \times 100\% \quad (3.1)$$

The *Misjudgment rates*（*M2*）indicate the proportion of the misjudged defects to the total number of detections.

$$M2 = \frac{DN\_sum + SD\_sum}{N\_sum} \times 100\% \quad (3.2)$$

The *Accuracy* represents the recognition rate and can be expressed as following:

$$Accuracy = 1 - M1 - M2 \quad (3.3)$$

Figure 3-1 illustrates some but common cases, where, the rectangles denote the detections produced by the system. In this paper, we mainly evaluate the performance of the recognition system by *M1* and *M2*.

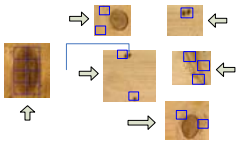

Figure 3-1. Some examples in the detection.

4 SVM classifier with typical features

4.1 Choose the training set and test sets

There are many kinds of defects and knots can often be seen and affect the quality and grading of woods. Here, we emphasize particularly on knots and some varieties of knots are shown in Figure 4-1. In the experiments, we select 2106 wood samples as the training set, including 1229 positive samples(labeled 1) and879 negative samples (labeled 0) from the knot image database provided by VTT Building Technology.

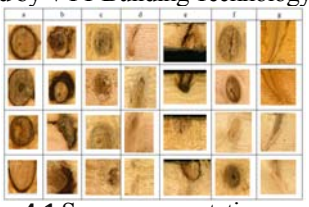

Figure 4-1. Some representative samples.

It is also an arduous task for us to select the test samples. In the experiments, we choose 30 representative samples as the test set named WDIT. Six images of WDIT named WDIT-1 are shown in Figure 4-2.

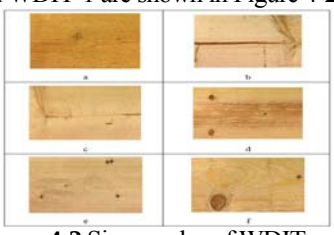

Figure 4-2. Six samples of WDIT.

4.2 Description recognition algorithm

recognition algorithm

1. (Input)

Training set are $\{(x_1,y_1),...,(x_n,y_n)\}$*, including DWT based p-dimension features and NMF based q- dimension features, where n=A+B, of which A is an aggregate of samples and have* $y_i = 0$*, and B is an aggregate of normal samples and have* $y_i = 1$*;*

2. (Initialization)

Scale the training set to [-1, 1];

Select the best kernel parameters C and gamma;

Train a SVM model and a hyper-plane $(w^* \bullet x_i) + b^* = 0$ *will be obtained. Finally, a decision- making function can be described as* $y = \mathrm{sgn}((w^* \bullet x_i) + b^*)$*.*

3. (Test and Output)

Load test sample T, cut T into many small blocks from the coordinates (0, 0) by step 30 pixels to the end and extracted the typical features from each small samples as the bases for recognition.

If the feature vectors distributed in the side of $(w^* \bullet x_i) + b^* \geq 1$*, then the pre-labels produced in the process of detection will be equal to zero and the algorithm will denote it automatically.*

The detailed wood defect recognition process is represented in Figure 4-3.

Figure 4-3. Wood defect recognition process.

5 Simulation and experiments

Some wood surfaces are relatively clean and the texture distribution is regular, however, in the actual production, most wood surfaces are not so smooth but blurry. Besides, large kinds of defects make the current methods fulfilled are unstable and vulnerable to the external interferences.

Before the experiments, we need obtain the best kernel parameters C and gamma by python and gnuplot. In the experiments, we mainly take WDIT as major experimental basis, of which the sample class distribution may be described in Table 5-1.

Table 5-1. Sample class distribution.

The types of Knots	Number of samples		Total
	Training set	Test set	
Dry knot	69	33	102
Encased knot	39	5	44
Decayed knot	14	7	21
Leaf knot	67	4	71
Edge knot	62	1	63
Sound knot	176	12	188
Horn knot	32	6	38
Total	459	68	527

The results will be used to evaluate the performance of the algorithm. This chapter mainly contains three main proportions. In order to highlight the superiority of USF-LDT, the sketch diagrams of detection and the distribution curves are given. Experimental tool:OSU_SVM;Experimental environment: Intel(R) Pentium(R) D CPU 2.80 GHz 2.79 GHz 512 M

5.1 Comparative test one

Here, we actualize the wood defect recognition method based on LBP with SVM classifier. The detailed test results based on WDIT-1 are recorded and shown in Table 5-2. The remaining test results of the other wood images were not individually given here. Through the test results, we summarized the problems encountered and the limitations itself to judge whether the proposed method has better robustness.

Table 5-2. The test results of LBP +SVM arithmetic on WDIT-1.

samples	Method (C=12,gamma= 0.001)	*false decision*		Missed rates		Accuracy	
		R-sum	Q-sum	N_dlabeled	N_labeled	N_sum	Statistical data
Sample1	LBP+SVM	0	2	1	1	192	98.96%
Sample2	LBP+SVM	12	16	2	3	192	52.08%
Sample3	LBP+SVM	0	2	1	1	160	98.75%
Sample4	LBP+SVM	0	2	3	3	192	98.96%
Sample5	LBP+SVM	2	6	3	4	154	69.81%
Sample6	LBP+SVM	0	9	2	2	176	94.89%
The rest	LBP+SVM	/	/	/	/	/	Average: 88.24%

5.1.1 Performances of SVM classifier with DTCWT features

In this section, we realize the recognition technology based on DTCWT with SVM classifier. Similarly, the test results based on WDIT-1 are recorded. After the tests, we will analyze the results earnestly and sum up the shortages of the features extracted by DTCWT. The detailed test results based on WDIT-1 are given in Table 5-3.

Table 5-3. The test results of DTCWT+SVM arithmetic on WDIT-1.

samples	Method (C=800,gamma =500)	*false decision*		Missed rates		Accuracy	
		R-sum	Q-sum	N_dlabeled	N_labeled	N_sum	Statistical data
Sample1	DTCWT+SVM	1	12	1	1	192	93.23%
Sample2	DTCWT+SVM	6	4	3	3	192	94.79%
Sample3	DTCWT+SVM	2	7	1	1	160	94.37%
Sample4	DTCWT+SVM	0	3	3	3	192	98.44%
Sample5	DTCWT+SVM	0	2	4	4	154	98.96%
Sample6	DTCWT+SVM	0	5	2	2	176	97.16%
The rest	DTCWT+SVM	/	/	/	/	/	Average: 92.14%

5.1.2 Performances of SVM classifier with the typical features

Here, we implement recognition technology based on the typical features USF-LDT with SVM classifier. Analogously, the test results based on WDIT-1 were recorded. The Detailed test results are shown in Table 5-4.

Table 5-4. The test results of USF-LDT+ SVM arithmetic on WDIT-1

samples	Method (C=12,gamma =100)	*false decision*		Missed rates		Accuracy	
		R-sum	Q-sum	N_dlabeled	N_labeled	N_sum	Statistical data
Sample1	USF-LDT+SVM	0	0	1	1	192	100%
Sample2	USF-LDT+SVM	0	3	3	3	192	98.44%
Sample3	USF-LDT+SVM	0	1	1	1	160	99.38%
Sample4	USF-LDT+SVM	0	0	3	3	192	100%
Sample5	USF-LDT+SVM	0	0	4	4	154	100%
Sample6	USF-LDT+SVM	0	1	2	2	176	99.43%
The rest	USF-LDT+SVM	/	/	/	/	/	Average: 95.63%

5.1.3 Contrast

In this section, we compare the three methods from two aspects: on the one hand, we compare the test results based by the diagrams shown in Figure 5-1, each column of which represents the results respectively; On the other hand, we will portray the distribution curves of the check items shown in Figure 5-2.

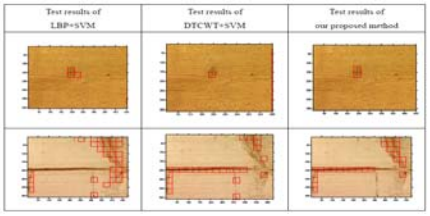

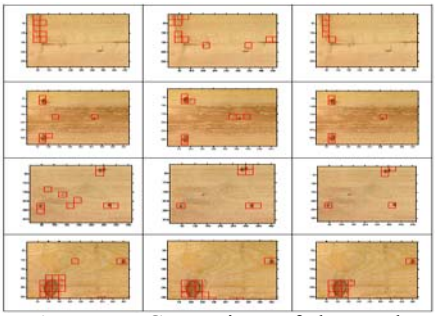

Figure 5-1. Comparison of the results of the three methods based on WDIT-1

Next, the distribution curves based on the different detection items were given, where, the blue lines represented USF-LDT+SVM method, the red lines represent LBP+SVM and the pink lines is DTCWT +SVM.

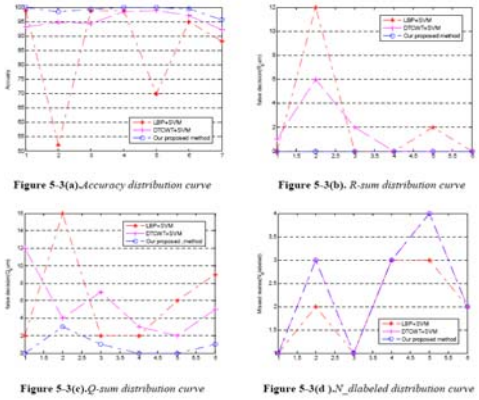

Figure 5-2. Distribution curve comparison.

Figure 5-3 depicts the curves of the three defect detection methods on WDIT. Next, the detailed analysis of the curves is given as following:

(1)From **Figure 5-2(a),** accuracy of our proposed method is better than DTCWT +SVM or LBP+SVM and has better stabilities;

(2) From **Figure 5-2(b) and Figure 5-2(c)**, the curve of our proposed method lies in below those of LBP+SVM and DTCWT+SVM, indicating the errors reach the lowest;

(3) From **Figure 5-2(d)**, the curves of our proposed method and DTCWT+SVM are the same, illuminating that there are no missed situations appear;

The compared results showed the overall performance of our proposed technology is superior to others and has better robust to the disturbed information with good practical and promotional values.

5.2 Comparative test two

Here, we analyzed the performance of the three methods to give prominence to our proposed method. We don't think about the number of R_sum, Q_sum and N_dlabeled but turn to judge whether the methods can detect and carve the defects by the error that is the proportion of the number of the missed defects in detection to the total of the knots.

Table 5-4 describes the detailed test results respectively.

Table 5-5. Results of the system on WDIT.

Knots / Test results	Dry	Encased	Decayed	Leaf	Edge	Sound	Horn	Test results on WOOD_T (%)	
								LBP +SVM	DTCWT +SVM
Dry knot	33	0	0	0	0	0	0	8.3	9.5
Encased knot	0	5	0	0	0	0	0	9.1	8.7
Decayed knot	0	0	7	0	0	0	0	23.4	14.9
Leaf knot	0	0	0	4	0	0	0	7.8	15.5
Edge knot	0	0	0	0	1	0	0	9.5	10.8
Sound knot	0	0	0	0	0	12	0	11.4	16.4
Horn knot	0	0	0	0	0	0	6	9.2	8.3
The test results of our proposed method	7.6	8.3	11.1	6.9	8.8	10.0	8.0	78.7 / 60.7	84.1 / total

From Table 5-5, the accuracy of the proposed method reach more than 90%, suggesting the system can follow the manual classification even though there are some errors in the detection and recognition.

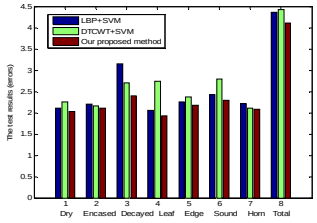

Figure 5-3.The plot diagrams of the results.

Figure 5-3 depicts the bar diagrams of the results in the log-form on WDIT, where the curve of our proposed method is lower than the others, which demonstrates that it has better detection ability to knots.

6 Conclusions and Outlooks

Conclusions.

The main purpose of this paper is to present a new wood defect recognition method. Moreover, the results of our proposed method presented here were good or considerably better than the results obtained by the other two methods. The experimental results show our proposed method has better robust to the interferences.

Though this technology has made a better recognition result, it is still in further study. At present, it has a certain distance from being applied to the actual production. However, it has perfect theoretical foundation and technology feasibility. Finally, we will receive a better recognition effect, meeting the strict requirements of the l production to a certain extent.

Outlooks.

Later, we will continue doing the following tasks well：(1) Improve the recognition algorithm further and effectively heighten the accuracy. And we will study the "defects overlapping" problems；(2) Considering the varieties of knots, convert the original problem into multi-class identification problem. After the recognition algorithm was mature, we will improve the system further and the image scanning and capture technology will be introduced to implement real-time detection.

Acknowledgements.

We will thank VTT Building Technology for supplying us with the wood image database and the wood knot database along with their invaluable contributions. Moreover, this research is supported by the National Science Foundation of China No. 30671639, the Natural Science Foundation of JiangSu province in China No. BK2005134 and the College Undergraduate Innovation Training Program 2008 of JiangSu Province in China.

References

[1]Matti Niskanen, Olli Silv, and Hannu Kauppinen,Machine Vision and Intelligent Syestem Group. Color and textur based wood inspection with nonsupervised clustering, Machine Vision and Applicati ons, 275–285:2003.

[2]P.Meinlschmidt, Wilhelm-Klauditz-Institut(WKI), Fraunhofer-Institute for wood research, Braunsch weig, Thermo-graphic detection of defects in wood and wood- based materials.14th international Symposium of nondestructive testing of wood, Hannover, Germany: May 2nd -4th ,2005

[3]Mäenpää T&Pietikäinen, M. Texture Analysis with Local Binary Patterns. In: Chen, C.H., Wang, P.S.P. (eds.): Handbook of Pattern Recognition and Computer Vision, 3rd ed. World Scientific 197-216: 2004

[4]Ojala T, Pietikäinen M & Mäenpää TMulti-resolution gray-scale and rotation invariant texture classification with local binary patterns. IEEE Transactions on Pattern Analysis and Machine Intelligence, 24(7), 971-987: 2002.

[5]N. G. Kingsbury. Shift invariant prosperities of the dual-tree complex wavelet transform. IEEE Icassp'99, Phoenix, AZ, 1999.

[6]N. G. Kingsbury, Image Processing with Complex Wavelet, Philos, Trans, Rov, So c London Ser, A, 357, 2543-2560. 1999.

[7]Kingsbury N G. The dual-tree complex wavelet transform: a new technique for shift variance and directional filter [R] . In Proc. of the IEEE Digital Signal Processing Workshop, Bryce Canyon UT, USA , 1998.

[8]Kingsbury N G. Complex wavelets for shift invariant analysis and filtering of singnal [J]. Journal of Applied and Computational Harmonic Analysis, 10(3), 234: 2001.

[9]Ojala T, Pietikäinen, M & Harwood D.A comparative study of texture measures with classification based on features distribute ons. Pattern recognition 2 9. 199 6: 51-59.

[10]Tianhorng Chang, J ay Kuo C C. Texture analysis and classification with tree structured wavelet transform [A]. Image Processing, IEEE Transactions, 1993, 2 (4): 429-441.

[11]Magarey J, Kingsbury N. Motion estimation using a complex valued wavelet transform [A]. Signal Processing, IEEE Transactions, Issue: 4[C]. 1998, 46 :1069-1084.

[12]Serkan Hatipoglu, MitraS K. Texture feature extraction using teager filters and singular value decomposition [A]. Proc of IEEE Conference on Consumer Electronics [C]. 1998, 440- 441.